Elliptic Flow of Protons and Antiprotons in Au+Au Collisions at $\sqrt{s_{NN}}$ = 7.7–62.4 GeV within Alternative Scenarios of Three-Fluid Dynamics

Yu.B. Ivanov[1, *]

[1] *Kurchatov Institute, Moscow RU-123182, Russia*

Analysis of elliptic flow of protons and antiprotons in Au+Au collisions is performed in a wide range of incident energies $\sqrt{s_{NN}}$ = 7.7–62.4 GeV. Simulations has been done within the three-fluid model employing a purely hadronic equation of state (EoS) and two versions of the EoS involving deconfinement transition: an EoS with the first-order phase transition and that with a smooth crossover transition. It is found that the proton data are reproduced approximately to the same extent within all of the scenarios, including the hadronic one, while the deconfinement scenarios look certainly preferable for the antiproton elliptic flow. The fact that difference between elliptic flows of protons and antiprotons decreases with the incident energy rise is a consequence of reducing baryon stopping rather than an onset of deconfinement.

PACS numbers: 25.75.-q, 25.75.Nq, 24.10.Nz
Keywords: relativistic heavy-ion collisions, elliptic flow, hydrodynamics, deconfinement

I. INTRODUCTION

The large azimuthal anisotropic flow at the Relativistic Heavy Ion Collider (RHIC) is believed to be a conclusive evidence for the creation of dense partonic matter in ultra-relativistic nucleus-nucleus collisions. This anisotropy is described by flow parameters defined as the proper Fourier coefficients v_n of the particle distributions in azimuthal angle with respect to the reaction plane [1]. The major bulk of research both theoretical and experimental has been done on the elliptic flow (v_2).

Recently new data of the STAR Collaboration [2] on transverse-momentum dependence of the elliptic flow of identified particles in the incident energy range of $\sqrt{s_{NN}}$ = 7.7–62.4 GeV were reported. These data were taken within the Beam Energy Scan (BES) program proposed at RHIC. The BES program was proposed in order to study possible onset of deconfinement, as well as possibly to identify the location of the critical end point that terminates the crossover transition at small quark-chemical potential to a first-order phase transition at higher quark-chemical potential [3].

This work aims to analyze the new STAR data [2] within different scenarios (with and without deconfinement) of heavy-ion collisions in order to draw conclusions on the matter produced in these collisions. The simulations were performed within a model of the three-fluid dynamics (3FD) [4] employing three different equations of state (EoS): a purely hadronic EoS [5] (hadr. EoS) and two versions of EoS involving the deconfinement transition [6]. These two versions are an EoS with the first-order phase transition (2-phase EoS) and that with a smooth crossover transition (crossover EoS). Details of these calculations are described in Ref. [7]. First results of the 3FD simulations within alternative scenarios of heavy-ion collisions are reported in Refs. [7–9] dedicated to analysis of the baryon stopping and particle production. Results on transverse flow in the energy range of AGS (Alternating Gradient Synchrotron) and SPS (Super Proton Synchrotron) but only within hadronic EoS were presented in Refs. [10, 11].

The 3FD model [4] treats the process of a nuclear collision from the very beginning, i.e. from the stage of incident cold nuclei, to the final stage of freeze-out. Contrary to the conventional hydrodynamics, where local instantaneous stopping of projectile and target matter is assumed, a specific feature of the 3FD is a finite stopping power resulting in a counter-streaming regime of leading baryon-rich matter. The basic idea of a 3-fluid approximation to heavy-ion collisions [12–14] is that at each space-time point a generally nonequilibrium distribution of baryon-rich matter can be represented as a sum of two distinct contributions initially associated with constituent nucleons of the projectile (p) and target (t) nuclei. In addition, newly produced particles, populating the mid-rapidity region, are associated with a fireball (f) fluid. Therefore, the 3-fluid approximation is a minimal way to simulate the finite stopping power at high incident energies.

The main observation of Ref. [2] is a strong difference in $v_2(p_t)$ between particles and their corresponding antiparticles. It is argued that it cannot be explained in a purely hydrodynamic approach since particles and anti-particles have the same mass. The evolution of the elliptic flow in the transient BES energy range was addressed in a number of theoretical works [15–20].

In Refs. [15, 16] the difference between particles and antiparticles is explained by the presence of a vector mean field potential which is repulsive for particles and attractive for antiparticles. In [15] it is introduced at the quark level within the Nambu-Jona-Lasinio (NJL) model, while in [16], at the hadronic level. As a consequence of these potentials, antiparticles are attracted by the matter and are trapped in the system, whereas particles feel a repulsive force and have the tendency to leave

*e-mail: Y.Ivanov@gsi.de

the system along the participant plane. With the potentials included, a fair qualitative agreement was achieved [16].

In Ref. [17], a hybrid (hydrodynamical plus Ultrarelativistic Quantum Molecular Dynamics [21]) calculation was performed. The effect for the protons-antiprotons primarily results from the annihilation process. Antiprotons moving in the out-of-plane direction encounter more protons to annihilate with than those moving in the in-plane direction. Another effect discussed in this paper is related to the event plane calculation. It was claimed that fluctuations in this calculation can bias the event plane to be rotated towards the most abundantly produced particles. This would, for example, increase the v_2 values for protons and reduce them for anti-protons.

The 3FD model proposes a more plausible (as compared to Refs. [15, 16]) explanation of the difference between particle and antiparticle elliptic flow in terms of three interacting fluids: the fireball, consisting of particles newly produced near the spacial center of the colliding system, and two baryon-rich fluid (p and t) associated with leading particles which traversed the whole system and are finally located in longitudinally peripheral regions. The particle-antiparticle difference explained by the increase of nuclear stopping in heavy ion collisions with decreasing energy. When the nuclear stopping becomes strong, the mid-rapidity quantities are determined not only by particles newly produced near the spacial center (the f-fluid) but also contributed by leading particles (the p- and t-fluids). The center and peripheral regions differently contribute to the mid-rapidity elliptic flow of different species, because they have different content of particles-antiparticles (quarks-antiquarks). This naturally results in different v_2 of particles and antiparticles because the center and peripheral regions have different v_2 patterns. This explanation is similar in some features to those proposed in Refs. [18, 19]. Contrary to Refs. [18, 19], the 3FD model calculates contribution from peripheral regions, rather than does assumptions on them, and does not employs the quark coalescence.

II. COMPARISON WITH DATA

The elliptic flow is proportional to the spatial anisotropy [22, 23]. Usually, for this purpose one uses the eccentricity ε defined by

$$\varepsilon = \frac{\langle y^2 \rangle - \langle x^2 \rangle}{\langle y^2 \rangle + \langle x^2 \rangle} \,. \tag{1}$$

Mean values of spacial transverse coordinates $\langle x^2 \rangle$ (out of the reaction plane) and $\langle y^2 \rangle$ (in the reaction plane) are usually calculated with either the wounded-nucleon (WN) or the binary-collision (BC) weights, for details see Ref. [24]. These calculations are based on the usual Woods–Saxon profile of nuclear density

$$\rho(r) = \frac{\rho_0}{1 + \exp[(r - R_A)/d]}, \tag{2}$$

where ρ_0 is the normal nuclear density, $R_A = 1.12A^{1/3}$ is the raduis of a nucleus with mass number A, and d is a diffuseness of the nuclear surface.

As long as the eccentricity is small, elliptic flow should be directly proportional to the eccentricity. For numerically large eccentricities the direct proportionality could break in principle, but as was shown in the very first hydrodynamic calculation by Ollitrault [22] the proportionality holds well even for rather large values of ε.

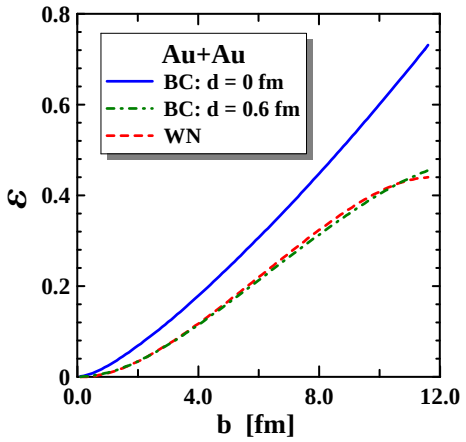

FIG. 1: Spatial eccentricity ε as a function of impact parameter in Au+Au collisions for different surface diffusenesses of the Au nucleus (d) and different weights of averaging: the wounded-nucleon (WN) and the binary-collision (BC) weights [24].

Within the 3FD model the initial nuclei are represented by sharp-edged spheres, i.e. the zero diffuseness ($d = 0$). This is done for stability of the incident nuclei before collision. This circumstance essentially affects the eccentricity. The results obtained with $d = 0$ and the realistic value of $d = 0.6$ fm calculated with BC weights are shown in Fig. 1. As seen, the ($d = 0$)-result noticeably exceeds the eccentricity for the physically realistic value of $d = 0.6$ fm. Moreover, the ($d = 0.6$ fm)-result with BN weights practically coincides with the eccentricity calculated with WN weights. The latter is considered as a realistic eccentricity and is accepted in the experimental analysis Ref. [24].

The overestimation of ε in the 3FD model naturally results in the respective overestimation of the elliptic flow. There are two ways to compensate this overestimation: either the impact parameter of the collision should be reduced to get a reasonable value of ε for a considered centrality bin or the calculated value of v_2 should be rescaled with the factor of $\varepsilon_{BN}(d = 0.6 \text{ fm})/\varepsilon_{BN}(d = 0)$, because $v_2 \propto \varepsilon$, as mentioned above. The latter method is applied in this paper, i.e. all the v_2 values displayed below are rescaled with the above factor. As the calculations

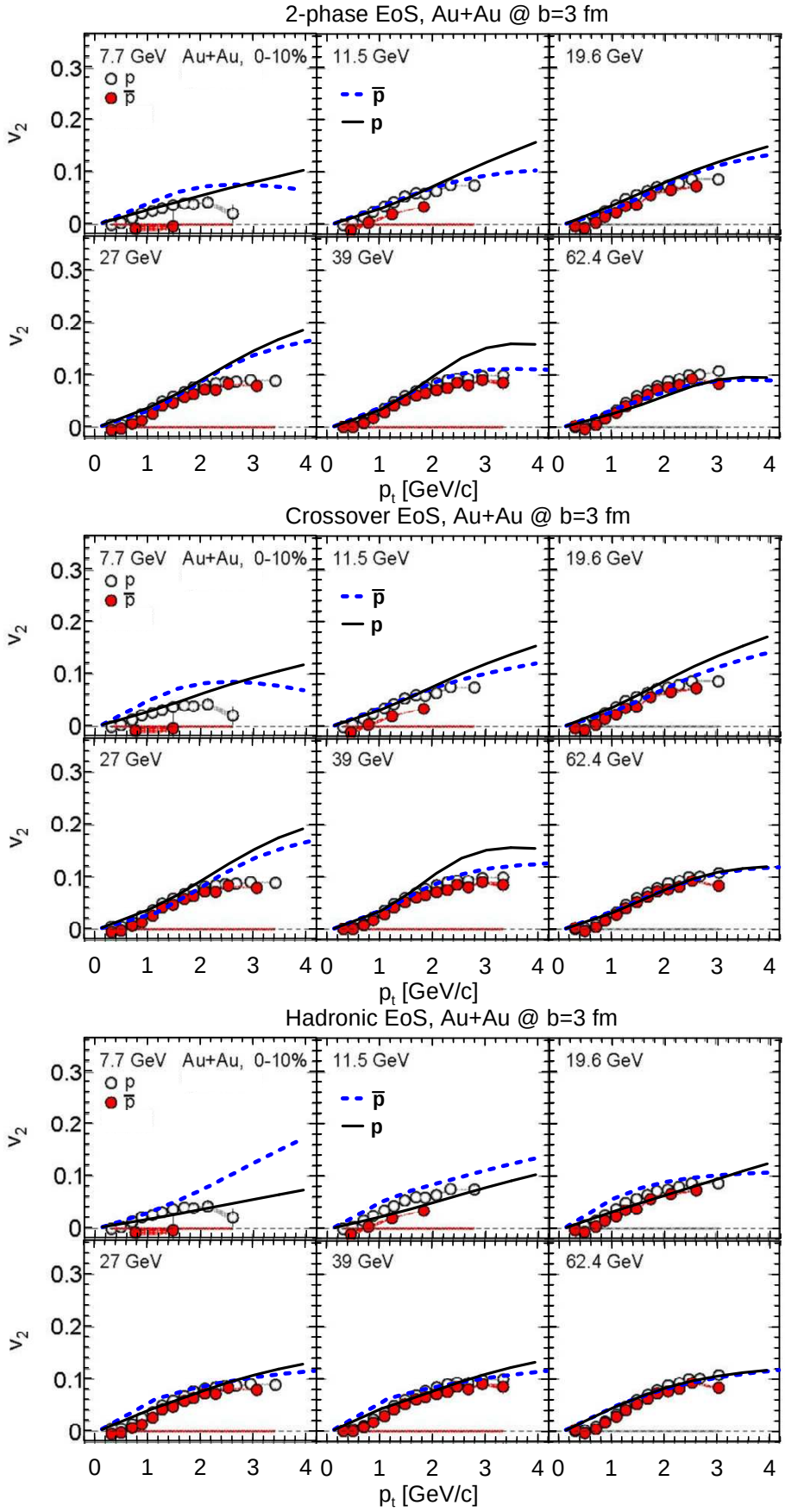

FIG. 2: Elliptic flow of protons and antiprotons at mid-rapidity in central (0%-10%) Au+Au collisions at $\sqrt{s_{NN}}$ = 7.7, 11.5, 19.6, 27, 39 and 62.4 GeV as a function of transverse momentum. The 3FD calculations are performed at b = 3 fm. Experimental data are from Star Collaboration [2].

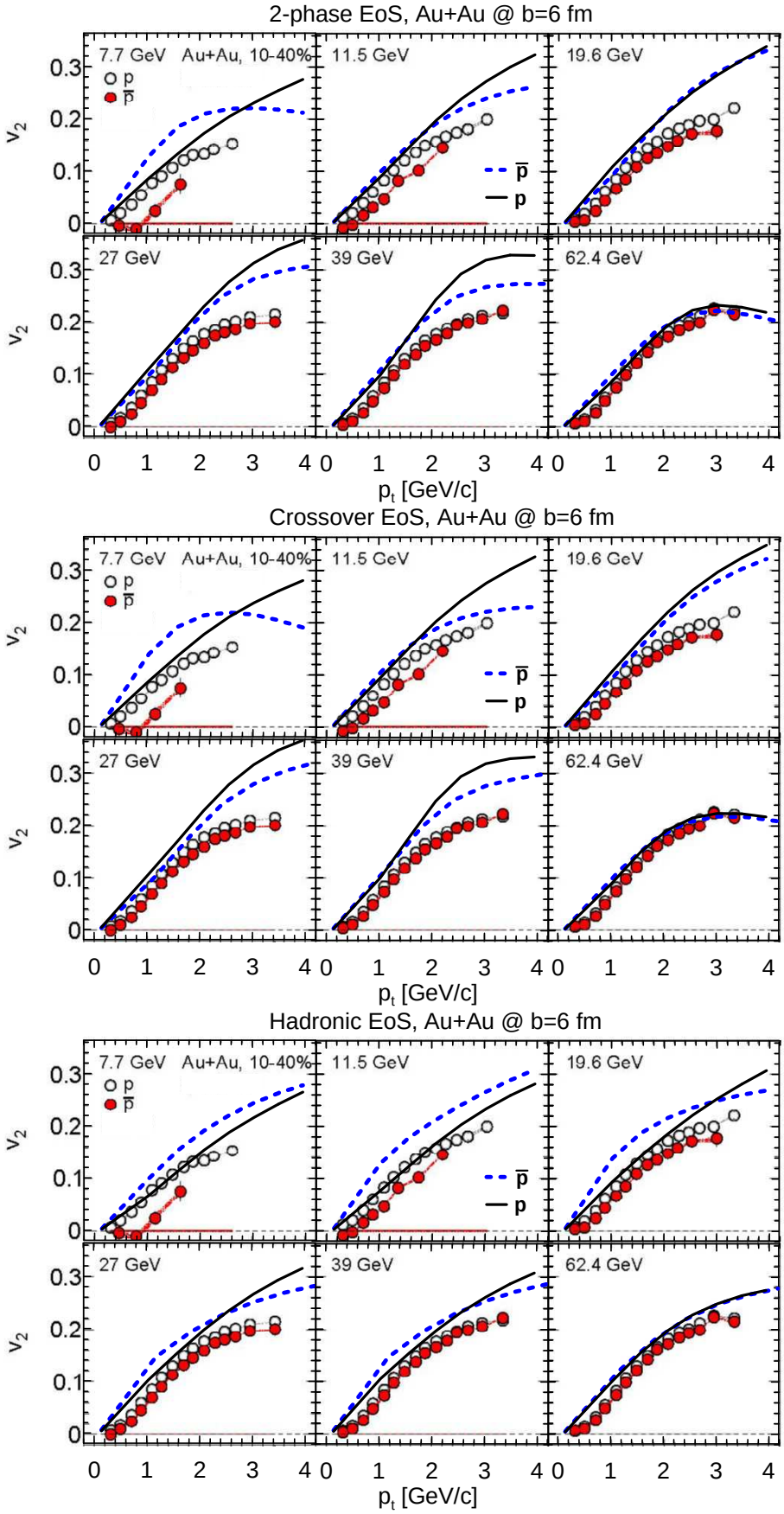

FIG. 3: The same as in Fig. 2 but for mid-central (10%-40%) Au+Au collisions. The 3FD calculations are performed at $b =$ 6 fm.

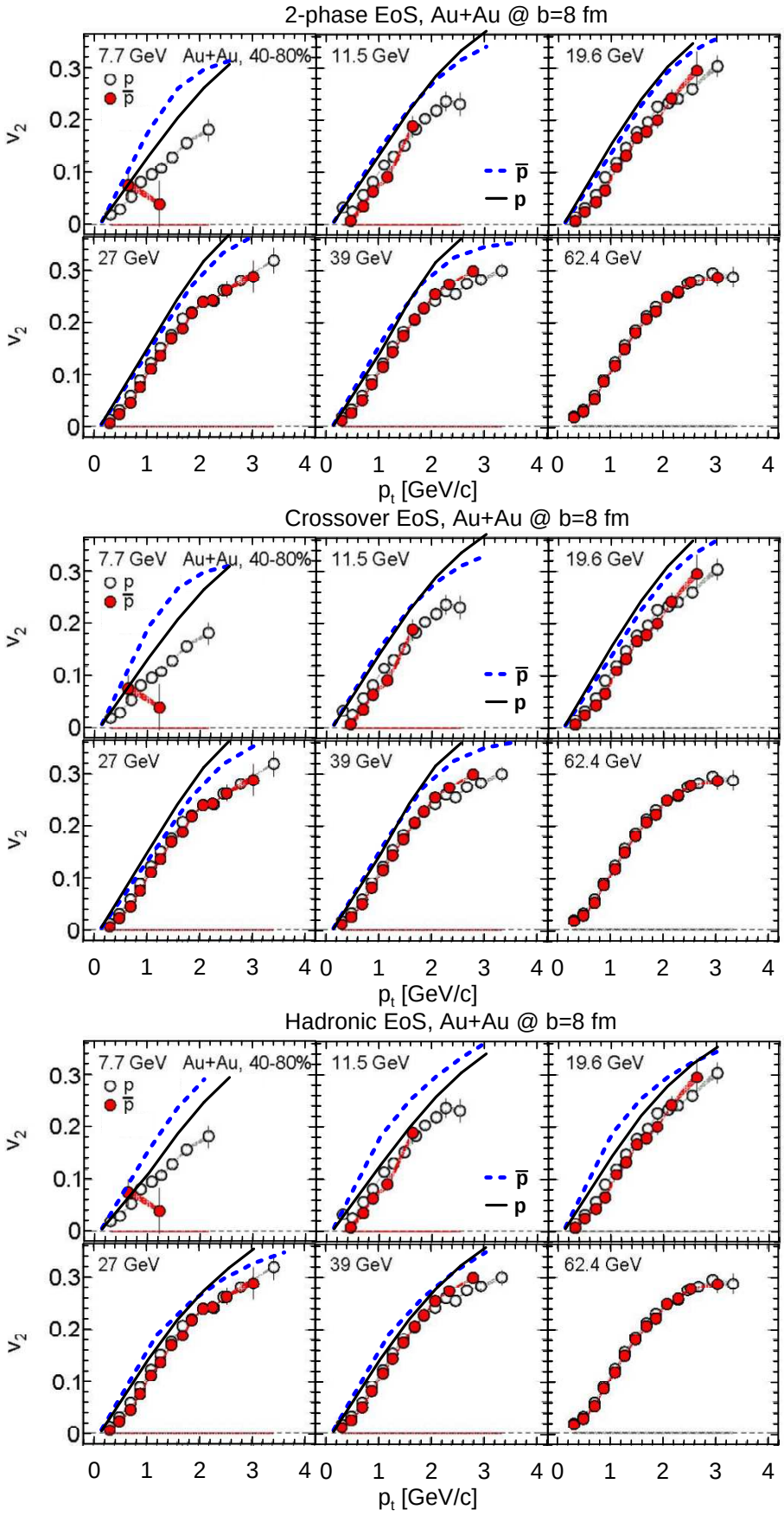

FIG. 4: The same as in Fig. 2 but for peripheral (40%-80%) Au+Au collisions. The 3FD calculations are performed at $b = 8$ fm.

are performed at fixed impact parameters, only proton and antiproton elliptic flow is considered for which data with comparatively narrow centrality selection are available [2].

Results of calculations of proton and antiproton elliptic flow at mid-rapidity and their comparison with STAR data [2] for three centrality bins are presented in Figs. 2, 3 and 4. The quality of data reproduction is quite reasonable for calculations at fixed impact parameters that are representative for the centrality bins considered. It should be kept in mind that in spite of the best reproduction at the top considered energy of 62.4 GeV, results at this energy are still not quite accurate, since an accurate computation requires unreasonably high memory and CPU time. Precisely due to this reason the calculations of peripheral ($b = 8$ fm) collisions at 62.4 GeV have not been done.

All scenarios, including the purely hadronic one, quantitatively reproduce the proton data approximately to the same extent. It simply means that all scenarios represent strongly collective (fluid-like) behavior of the system that results in a large elliptic flow. The value of v_2 does not directly indicate either hadronic or partonic content of the matter. To distinguish between the hadronic and partonic content we need more delicate properties of the elliptic flow. The calculated results as a rule overestimate the data. This makes room for the viscosity and/or afterburner corrections to the calculated results. In the 3FD model neither viscosity nor kinetic afterburner at the final stage of the expansion were incorporated.

Elliptic flows of protons and antiprotons at mid-rapidity coincide only if these are formed by the single fireball fluid, i.e. if baryon-rich fluids (the projectile and target ones) are well separated from the fireball fluid in rapidity. As seen this is almost the case at 62.4 GeV. With the incident energy decrease this separation in rapidity space becomes smaller, and as a result the the proton and antiproton v_2 differ from each other more and more. This is a consequence of difference in proton and antiproton content and in the v_2 patters of the baryon-rich and fireball fluids. Of course, exceptions from this rule are possible if v_2 patters of different fluids turn out to be very similar by some reason. For instance, this is the case for the energy of 19.6 GeV within deconfinement scenarios. Typically, v_2 of protons and antiprotons become closer to each other with the incident energy rise, similarly to that observed in the experiment. This takes place for all considered scenarios because the baryon-rich and fireball fluids get more and more separated in rapidity.

As for more delicate properties of the elliptic flow mentioned above, contrary to the hadronic scenario, all deconfinement scenarios result in proton elliptic flow exceeding or being approximately equal (with accuracy of the calculation) the antiproton one (with the exception of the lowest considered incident energy of 7.7 GeV). The latter is in qualitative agreement with the data. The lowest energy of 7.7 GeV is already quite close to onset of deconfinement within 2-phase-EoS and crossover-EoS scenarios [7, 8]. Therefore, the model predicts a kind of irregular behavior in this energy region that does not agree with the data at present. Within deconfinement scenarios the antiproton v_2 data are, as a rule, better reproduced in the low-momentum region, that is the prime region of the applicability of the fluid description. This indicates the preference of the deconfinement scenarios.

III. CONCLUSIONS

The elliptic flow of produced particles is one of the most sensitive observables that brings information about the degree of collectivity during the expansion stage of heavy-ion collisions. When the collectivity is strong, like in the case of ideal hydrodynamics, the elliptic flow takes the highest value (the so called hydrodynamic limit). If the collectivity is weak, like in a dilute system of weakly interacting particles, it is close to zero. The value of v_2 does not directly indicate either hadronic or partonic content of the matter. This is confirmed by approximately the same extent of reproduction of the proton and antiproton elliptic flow achieved within all scenarios, including the purely hadronic one.

To distinguish between the hadronic and partonic content we need more delicate properties of the elliptic flow. An indication in favor of the deconfinement scenarios is better reproduction of the antiproton elliptic flow in the low-momentum region within these scenarios because this region is the main domain of the applicability of the fluid description.

In the present version of the 3FD model neither viscosity nor kinetic afterburner at the final stage of the expansion are incorporated. Therefore, it is not surprising that the calculated elliptic flow, as a rule, overestimates the data. This makes room for the viscosity and/or afterburner corrections to the calculated results.

The calculated elliptic flows of protons and antiprotons become closer to each other with the incident energy rise, similarly to that observed in the experiment. In fact, the elliptic flows of protons and antiprotons at mid-rapidity coincide only if these are formed by a single fluid, expanding in the center of the colliding system, in other words, if this "center" fluid is well separated in rapidity from projectile- and target-like leading particles, dominantly occupying peripheral rapidity regions. If the nuclear stopping rises, as it takes place with incident energy decrease, the rapidity gap between the "center" fireball and the leading-particles matter shrinks. Then the leading-particles matter starts to contribute to the mid-rapidity quantities. In its turn, this results in a difference between elliptic flows of protons and antiprotons that is a consequence of difference in proton and antiproton content and in the v_2 patters of the "center" fireball and the leading-particles matter. In the 3FD model this mechanism is realized in terms of three interacting fluids: the fireball one, consisting of particles newly produced

near the spacial center of the colliding system, and two baryon-rich fluid (p and t) associated with leading particles which traversed the whole system and are finally located in longitudinally marginal regions.

Acknowledgements

I am grateful to A.S. Khvorostukhin, V.V. Skokov, and V.D. Toneev for providing me with the tabulated 2-phase and crossover EoS's. The calculations were performed at the computer cluster of GSI (Darmstadt). This work was supported by The Foundation for Internet Development (Moscow) and also partially supported by the Russian Ministry of Science and Education grant NS-215.2012.2.

[1] S. Voloshin and Y. Zhang, Z. Phys. C **70**, 665 (1996) [hep-ph/9407282].
[2] L. Adamczyk *et al.* [STAR Collaboration], arXiv:1301.2348.
[3] M. M. Aggarwal *et al.* [STAR Collaboration], arXiv:1007.2613 [nucl-ex].
[4] Yu. B. Ivanov, V. N. Russkikh, and V.D. Toneev, Phys. Rev. C **73**, 044904 (2006) [nucl-th/0503088].
[5] V. M. Galitsky and I. N. Mishustin, Sov. J. Nucl. Phys. **29**, 181 (1979).
[6] A. S. Khvorostukhin, V. V. Skokov, K. Redlich, and V. D. Toneev, Eur. Phys. J. **C48**, 531 (2006) [nucl-th/0605069].
[7] Yu. B. Ivanov, arXiv:1302.5766 [nucl-th], to be published in Phys. Rev. C.
[8] Yu. B. Ivanov, Phys. Lett. **B721**, 123 (2013) [arXiv:1211.2579 [hep-ph]].
[9] Yu. B. Ivanov, arXiv:1304.1638 [nucl-th].
[10] V. N. Russkikh and Yu. B. Ivanov, Phys. Rev. C **74** (2006) 034904 [nucl-th/0606007].
[11] Yu. B. Ivanov, I. N. Mishustin, V. N. Russkikh, and L. M. Satarov, Phys. Rev. C **80**, 064904 (2009) [arXiv:0907.4140 [nucl-th]].
[12] Y. .B. Ivanov, Yad. Fiz. **46**, 100 (1987) [Sov. J. Nucl. Phys. **46**, 63 (1987)].
[13] Yu.B. Ivanov, Nucl. Phys. **A474**, 669 (1987).
[14] I.N. Mishustin, V.N. Russkikh, and L.M. Satarov, Yad. Fiz. **54**, 429 (1991) [Sov. J. Nucl. Phys. **54**, 260 (1991)].
[15] T. Song, S. Plumari, V. Greco, C. M. Ko and F. Li, arXiv:1211.5511 [nucl-th].
[16] J. Xu, L. -W. Chen, C. M. Ko and Z. -W. Lin, Phys. Rev. C **85**, 041901 (2012) [arXiv:1201.3391 [nucl-th]].
[17] J. Steinheimer, V. Koch and M. Bleicher, Phys. Rev. C **86**, 044903 (2012) [arXiv:1207.2791 [nucl-th]].
[18] J. C. Dunlop, M. A. Lisa and P. Sorensen, Phys. Rev. C **84**, 044914 (2011) [arXiv:1107.3078 [hep-ph]].
[19] V. Greco, M. Mitrovski and G. Torrieri, Phys. Rev. C **86**, 044905 (2012) [arXiv:1201.4800 [nucl-th]].
[20] V. P. Konchakovski, E. L. Bratkovskaya, W. Cassing, V. D. Toneev, S. A. Voloshin and V. Voronyuk, Phys. Rev. C **85**, 044922 (2012) [arXiv:1201.3320 [nucl-th]].
[21] S. A. Bass, M. Belkacem, M. Bleicher, M. Brandstetter, L. Bravina, C. Ernst, L. Gerland and M. Hofmann *et al.*, Prog. Part. Nucl. Phys. **41**, 255 (1998) [nucl-th/9803035].
[22] J. Y. Ollitrault, Phys. Rev. D **46**, 229 (1992).
[23] S. A. Voloshin, A. M. Poskanzer and R. Snellings, arXiv:0809.2949 [nucl-ex].
[24] P. Jacobs and G. Cooper, arXiv:nucl-ex/0008015.